

PM-98/44
December 1998

Top Squark Effects on Higgs Boson Production and Decays at the LHC

ABDELHAK DJOUADI

Laboratoire de Physique Mathématique et Théorique,
Université Montpellier II, F-34095 Montpellier Cedex 5, France.
E-mail: djouadi@lpm.univ-montp2.fr

ABSTRACT

In the Minimal Supersymmetric Standard Model, one of the scalar top quarks can be relatively light and its couplings to Higgs bosons strongly enhanced. I will discuss two consequences of this feature: 1) the effects of scalar top loops on the main production mechanism of the lightest Higgs boson at the LHC, the gluon-fusion mechanism $gg \rightarrow h$, and on the important decay channel into two photons $h \rightarrow \gamma\gamma$; and 2) the production of the light Higgs particle in association with top-squark pairs at proton colliders, $pp \rightarrow \tilde{t}_1 \tilde{t}_1 h$.

Talk given at the Workshop RADCOR'98, Barcelona, Spain, September 1998.

Top Squark Effects on Higgs Boson Production and Decays at the LHC

Abdelhak DJOUADI

*Laboratoire de Physique Mathématique et Théorique,
Université Montpellier II, F-34095 Montpellier Cedex 5
E-mail: djouadi@lpm.univ-montp2.fr*

In the Minimal Supersymmetric Standard Model, one of the scalar top quarks can be relatively light and its couplings to Higgs bosons strongly enhanced. I will discuss two consequences of this feature: 1) the effects of scalar top loops on the main production mechanism of the lightest Higgs boson at the LHC, the gluon-fusion mechanism $gg \rightarrow h$, and on the important decay channel into two photons $h \rightarrow \gamma\gamma$; and 2) the production of the light Higgs particle in association with top-squark pairs at proton colliders, $pp \rightarrow \tilde{t}_1 \tilde{t}_1 h$.

1 Physical Set-Up

One of the main motivations of supersymmetric theories is the fact that they provide an elegant way to break the electroweak symmetry and to stabilize the huge hierarchy between the GUT and Fermi scales¹. The probing of the Higgs sector of the Minimal Supersymmetric Standard Model (MSSM)² is thus of utmost importance and the search for the neutral h, H and A and charged Higgs particles H^\pm of the MSSM is therefore one of the main entries in the present and future high-energy colliders agendas.

In the theoretically well motivated models, such as the mSUGRA scenario, the MSSM Higgs sector is in the so called decoupling regime³ for most of the SUSY parameter space allowed by present data constraints⁴: the heavy CP-even, the CP-odd and the charged Higgs bosons are rather heavy and almost degenerate in mass, while the lightest neutral CP-even Higgs particle reaches its maximal allowed mass value $M_h \lesssim 80\text{--}130$ GeV⁵ depending on the SUSY parameters. In this scenario, the h boson has almost the same properties as the SM Higgs boson and would be the sole Higgs particle accessible at the next generation of colliders.

At the LHC, the most promising channel^{6,7} for detecting the lightest h boson is the rare decay into two photons, $h \rightarrow \gamma\gamma$ ⁸, with the Higgs particle dominantly produced via the top quark loop mediated gluon-gluon fusion mechanism⁹, $gg \rightarrow h$. In the decoupling regime, the two LHC collaborations expect to detect the narrow $\gamma\gamma$ peak in the entire Higgs mass range, $80 \lesssim M_h \lesssim 130$ GeV, with an integrated luminosity $\int \mathcal{L} \sim 300$ fb⁻¹ corresponding to three years of LHC running⁶.

Two other channels can be used to detect the h boson in this mass range ⁷: the production in association with a W boson or in association with top quark pairs, $pp \rightarrow hW$ and $pp \rightarrow t\bar{t}h$, with the h boson decaying into 2 photons and the t quarks into b quarks and W bosons. Although the cross sections are smaller compared to the $gg \rightarrow h$ case, the background cross sections are also small if one requires a lepton from the decaying W bosons as an additional tag, leading to a significant signal. Furthermore, $\sigma(pp \rightarrow t\bar{t}h)$ is directly proportional to the top–Higgs Yukawa coupling, the largest electroweak coupling in the SM; this process would therefore allow the measurement of this parameter, and the experimental test of the fundamental prediction that the Higgs couplings to SM particles are proportional to the particle masses.

In this talk, I will discuss the effects of SUSY particles in the production of the lightest h boson at the LHC: first the contributions of light stops in the gluon-fusion mechanism $gg \rightarrow h$ and the $h \rightarrow \gamma\gamma$ decay ¹⁰ which can significantly alter the production rate, and then the associated production of the h boson with \tilde{t} -squark pairs, $pp \rightarrow \tilde{t}_1\tilde{t}_1h$ ¹¹, for which the cross section can be rather large, exceeding the one for the SM-like process $pp \rightarrow t\bar{t}h$.

One of the most important ingredients of these discussions is that stops can alter significantly the phenomenology of the MSSM Higgs bosons. The reason is two-fold: (i) the current eigenstates, \tilde{t}_L and \tilde{t}_R , mix to give the mass eigenstates \tilde{t}_1 and \tilde{t}_2 ; the mixing angle $\theta_{\tilde{t}}$ is proportional to $m_t A_t$ [$\tilde{A} = A_t - \mu/\tan\beta$ with A_t is the stop trilinear coupling, μ the higgsino mass parameter and $\tan\beta$ the ratio of the vev 's of the two Higgs doublets], and can be very large, leading to a scalar top squark \tilde{t}_1 much lighter than the t -quark and all other scalar quarks [note that the mixing in the sbottom sector can be also sizeable for large values of $\tan\beta, \mu$ and A ; however this will not be discussed here and the \tilde{b} mixing will be set to zero]; (ii) the couplings of the top squarks to the neutral Higgs bosons in the decoupling regime

$$g_{h\tilde{t}_1\tilde{t}_1} \propto -\cos 2\beta \left[\frac{1}{2} \cos^2 \theta_{\tilde{t}} - \frac{2}{3} s_W^2 \cos 2\theta_{\tilde{t}} \right] - \frac{m_{\tilde{t}}^2}{M_Z^2} + \frac{1}{2} \sin 2\theta_{\tilde{t}} \frac{m_t \tilde{A}_t}{M_Z^2} \quad (1)$$

involve components which are proportional to \tilde{A}_t and for large values of this parameter, the $g_{h\tilde{t}_1\tilde{t}_1}$ coupling can be strongly enhanced.

2 Higgs production in the gluon fusion mechanism

In the SM, the Higgs–gluon–gluon vertex is mediated by heavy [mainly top and to a lesser extent bottom] quark loops, while the rare decay into two photons is mediated by W -boson and heavy fermion loops, with the W -boson

contribution being largely dominating. In the MSSM however, additional contributions are provided by SUSY particles: \tilde{q} loops in the case of the hgg vertex, and H^\pm, \tilde{f} and χ^\pm loops in the case of the $h \rightarrow \gamma\gamma$ decay. In Ref. ⁸, it has been shown that only the contributions of relatively light \tilde{t} squarks [and to a lesser extent χ_1^\pm for masses close to 100 GeV, which could contribute at the 10% level] can alter significantly the loop induced hgg and $h\gamma\gamma$ vertices. The $\gamma\gamma$ and gg decay widths [the gg cross section is proportional to the partial width] of the h boson, including the SUSY loops and the QCD corrections, are evaluated numerically with the help of the program HDECAY ¹².

Figs. 1 and 2 show, as a function of \tilde{A}_t for $\tan\beta = 2.5$, the deviations from their SM values of the partial decay widths of the h boson into two photons and two gluons as well as their product which gives the cross section times branching ratio $\sigma(gg \rightarrow h \rightarrow \gamma\gamma)$. The quantities R are defined as the partial widths including, over the ones without [equivalent to SM in the decoupling limit] the SUSY loop contributions $R = \Gamma_{\text{MSSM}}/\Gamma_{\text{SM}}$.

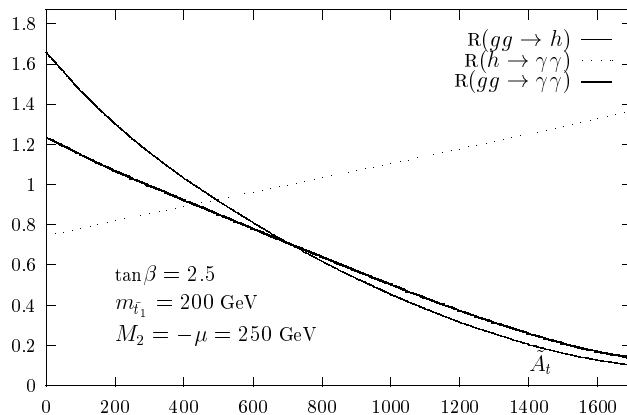


Figure 1: SUSY loop effects on $R(gg \rightarrow h)$, $R(h \rightarrow \gamma\gamma)$ and $R(gg \rightarrow \gamma\gamma)$ as a function of \tilde{A}_t for $\tan\beta = 2.5$ and $m_{\tilde{t}_1} = 200$ GeV, $M_2 = -\mu = 250$ GeV.

In Fig. 1, the stop mass is set to $m_{\tilde{t}_1} = 200$ GeV. For small values of \tilde{A}_t there is no mixing in the stop sector and the dominant component of the $h\tilde{t}\tilde{t}$ couplings eq. (1) is $\sim m_t^2/M_Z^2$. In this case, the t and \tilde{t} contributions interfere constructively in the hgg and $h\gamma\gamma$ amplitudes, which leads to an enhancement of the $h \rightarrow gg$ decay width and a reduction of the $h \rightarrow \gamma\gamma$ decay width [that is dominated by the W amplitude which interferes destructively with the t and \tilde{t} amplitudes]. The product $R(gg \rightarrow \gamma\gamma)$ in the MSSM is then enhanced by a factor ~ 1.2 in this case. With increasing \tilde{A}_t , the two components of $g_{h\tilde{t}_1\tilde{t}_1}$

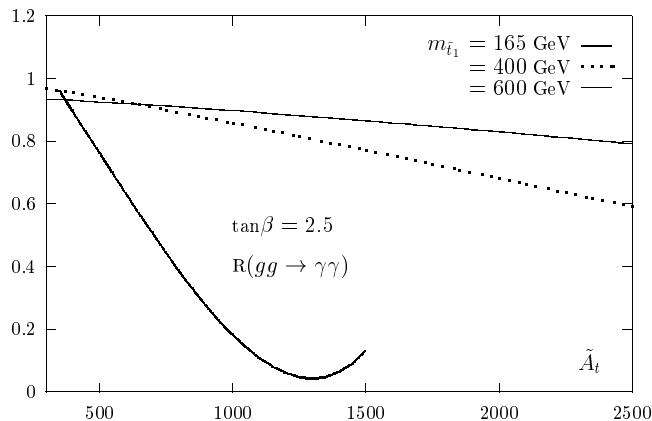


Figure 2: SUSY loop effects on $R(gg \rightarrow \gamma\gamma)$ as a function of \tilde{A}_t for $\tan\beta = 2.5$ and $m_{\tilde{t}_1} = 165, 400$ and 600 GeV with $M_2 = -\mu = 500$ GeV for $m_{\tilde{t}_1} \geq 400$ GeV.

interfere destructively and partly cancel each other, resulting in a rather small stop contribution. For larger values of \tilde{A}_t , the last component of $g_{h\tilde{t}_1\tilde{t}_1}$ becomes the most important one, and the \tilde{t}_1 loop contribution interferes destructively with the t -loop. This leads to an enhancement of $R(h \rightarrow \gamma\gamma)$ and a reduction of $R(gg \rightarrow h)$; however, the reduction of the latter is much stronger than the enhancement of the former and the product $R(gg \rightarrow \gamma\gamma)$ decreases with increasing \tilde{A}_t . For \tilde{A}_t values of about 1.5 TeV, the signal for $gg \rightarrow h \rightarrow \gamma\gamma$ in the MSSM is smaller by a factor of ~ 5 compared to the SM case.

Fig. 2 shows the deviation $R(gg \rightarrow \gamma\gamma)$ with the same parameters as in Fig. 1 but with different \tilde{t}_1 masses, $m_{\tilde{t}_1} = 165, 400$ and 600 GeV. For larger masses, the top squark contribution $\propto 1/m_{\tilde{t}_1}^2$, will be smaller than in the previous case. For $m_{\tilde{t}_1} \simeq 400$ GeV, the effect is less striking compared to the case of $m_{\tilde{t}_1} = 200$ GeV, since here $\sigma(gg \rightarrow h) \times \text{BR}(h \rightarrow \gamma\gamma)$ drops by less than a factor of 2, even for extreme values of $\tilde{A}_t \sim 2.5$ TeV. In contrast, if the stop mass is reduced to $m_{\tilde{t}_1} \simeq 165$ GeV, the drop in $R(gg \rightarrow \gamma\gamma)$ will be even more important: for $\tilde{A}_t \sim 1.5$ TeV, the $gg \rightarrow \gamma\gamma$ rate including stop loops is an order of magnitude smaller than in the SM. For $\tilde{A}_t \sim 1.3$ TeV, the \tilde{t} amplitude almost cancels completely the t/b quark amplitudes.

One should recall that M_h varies with \tilde{A}_t , and no constraint on M_h has been set in Figs. 1–2. Requiring $M_h \gtrsim 90$ GeV, the lower range $\tilde{A}_t \lesssim 350$ GeV and the upper ranges $\tilde{A}_t \gtrsim 1.5(2.3)$ TeV for $m_{\tilde{t}_1} = 200(400)$ GeV for instance, are ruled out. This means that the scenario where $R(gg \rightarrow \gamma\gamma) > 1$, which occurs only for $\tilde{A}_t \lesssim 300$ GeV for $m_{\tilde{t}_1} = 200$ GeV is ruled out for $M_h \gtrsim 90$

GeV. [Note also that despite of the large (\tilde{t}, \tilde{b}) mass splitting for large \tilde{A}_t values, the contributions of the isodoublet to electroweak observables¹³ stay below the experimentally acceptable level]. Therefore, the rate for the $gg \rightarrow \gamma\gamma$ process in the MSSM will always be smaller than in the SM case, making more delicate the search for the h boson at the LHC with this process.

3 Higgs production in association with light stops

If one of the stop squarks is light and its coupling to the h boson is enhanced, an additional process might provide a new important source for Higgs particles: the associated production with \tilde{t} states,

$$pp \rightarrow gg + q\bar{q} \rightarrow \tilde{t}_1\tilde{t}_1h \quad (1)$$

At lowest order, i.e. at $\mathcal{O}(G_F\alpha_s^2)$, the process is initiated by 12 Feynman diagrams. Due to the larger gluon luminosity at high energies, the contribution of the 10 gg -fusion diagrams is much larger than the contribution of the 2 $q\bar{q}$ annihilation diagrams at the LHC.

In Fig. 3, the $pp \rightarrow \tilde{t}_1\tilde{t}_1h$ cross section [in pb] is displayed as a function of $m_{\tilde{t}_1}$ for $\tan\beta = 2$, in the case of no-mixing [$A_t = 200, \mu = 400$ GeV], moderate mixing [$A_t = 500$ and $\mu = 100$ GeV] and large mixing [$A_t = 1.5$ TeV and $\mu = 100$ GeV]. We have used $m_{\tilde{t}_L} = m_{\tilde{t}_R} \equiv m_{\tilde{q}}$ as is approximately the case in GUT scenarios. Note for comparison, that the cross section for the standard-like $pp \rightarrow \bar{t}th$ process is of the order of 0.6 pb for $M_h \simeq 100$ GeV⁷; $m_t = 175$ GeV, and the CTEQ4 parameterizations of the structure functions¹⁴ are chosen for illustration.

If there is no mixing in the stop sector, \tilde{t}_1 and \tilde{t}_2 have the same mass and approximately the same couplings to the h boson since the m_t^2/M_Z^2 components are dominant. The cross section, which should be then multiplied by a factor of two to take into account both squarks, is comparable to the $\sigma(pp \rightarrow \bar{t}th)$ in the low mass range $m_{\tilde{t}} \lesssim 200$ GeV. [If the \tilde{t} masses are related to the masses of the light quark partners, $m_{\tilde{q}}$, the range for which the cross section is rather large is therefore ruled out by the experimental constraints on $m_{\tilde{q}}$.] For intermediate values of \tilde{A}_t the two components of the $h\tilde{t}_1\tilde{t}_1$ coupling interfere destructively and partly cancel each other, resulting in a rather small cross section, unless $m_{\tilde{t}_1} \sim \mathcal{O}(100)$ GeV. In the large mixing case $\tilde{A}_t \sim 1.5$ TeV $\sigma(pp \rightarrow \tilde{t}_1\tilde{t}_1h)$ can be very large. It is above the rate for the standard process $pp \rightarrow \bar{t}th$ for values of $m_{\tilde{t}_1}$ smaller than 220 GeV. If \tilde{t}_1 is lighter than the top quark, the $\tilde{t}_1\tilde{t}_1h$ cross section significantly exceeds the one for $\bar{t}th$ final states. For instance, for $m_{\tilde{t}_1} = 140$ GeV corresponding to $M_h \sim 76$ GeV, $\sigma(pp \rightarrow \tilde{t}_1\tilde{t}_1h)$ is an order of magnitude larger than $\sigma(pp \rightarrow \bar{t}th)$.

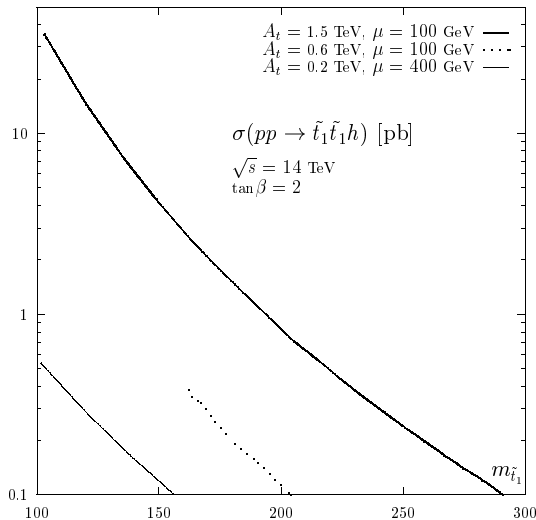


Figure 3: The production cross section $\sigma(pp \rightarrow \tilde{t}_1 \tilde{t}_1 h)$ [in pb] as a function of the \tilde{t}_1 mass and three sets of A_t and μ values and $\tan\beta$ is fixed to $\tan\beta = 2$.

In Fig. 4, we fix $m_{\tilde{t}_1} = 165 \text{ GeV} \sim m_t^{\overline{\text{MS}}}$ and display the $pp \rightarrow \tilde{t}_1 \tilde{t}_1 h$ cross section as a function of \tilde{A}_t . For comparison, the * and • give the standard-like $pp \rightarrow \bar{t} t h$ cross section for $M_h = 100 \text{ GeV}$ and $\tan\beta = 2$ and 30, respectively. For $\tan\beta = 30$ the cross section is somewhat smaller than for $\tan\beta = 2$, a mere consequence of the increase of the h boson mass with $\tan\beta$ ⁵. As can be seen again, the production cross section is substantial for the no-mixing case, rather small for intermediate mixing [becoming negligible for \tilde{A}_t values between 200 and 400 GeV], and then becomes very large exceeding the reference cross section for values of \tilde{A}_t above $\sim 1 \text{ TeV}$. For instance, for the inputs of Fig. 3, $\sigma(pp \rightarrow \tilde{t}_1 \tilde{t}_1 h)$ exceeds $\sigma(pp \rightarrow t \bar{t} h)$ in the SM for the same Higgs boson mass when $\tilde{A}_t \gtrsim 1(1.05) \text{ TeV}$ for $\tan\beta = 2(30)$.

For the signal, in most of the parameter space, the stop decay is $\tilde{t}_1 \rightarrow b\chi^+$ if $m_{\tilde{t}_1} < m_t + m_{\chi_1^0}$ where χ_1^0 is the LSP, or $\tilde{t}_1 \rightarrow t\chi_1^0$ in the opposite case. In the interesting region where $\sigma(pp \rightarrow \tilde{t}_1 \tilde{t}_1 h)$ is large, i.e. for light \tilde{t}_1 , the decay $\tilde{t}_1 \rightarrow b\chi^+$ is dominant, and the χ_1^+ will mainly decay into bW^+ + missing energy leading to $\tilde{t}_1 \rightarrow bW^+$ final states. This is the same topology as the decay $t \rightarrow bW^+$, except that in the case of the \tilde{t} there is a large amount of missing energy [if sleptons are also relatively light, charginos decays will also lead to $l\nu\chi_1^0$ final states]. The only difference between the final states generated by the $\tilde{t}\tilde{t}h$ and $t\bar{t}h$ processes, will be due to the softer energy spectrum of the charged leptons coming from the chargino decay in the former case, because of the

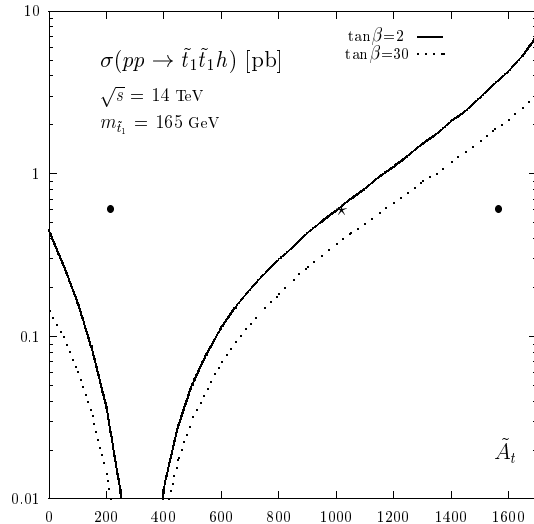


Figure 4: The production cross section $\sigma(pp \rightarrow \tilde{t}_1 \tilde{t}_1 h)$ [in pb] as a function as a function of \tilde{A}_t for fixed $m_{\tilde{t}_1} = 165$ GeV and for $\tan\beta = 2, 30$.

energy carried by the invisible LSP. The Higgs boson can be tagged through its $h \rightarrow \gamma\gamma$ decay mode; as discussed previously this mode can be substantially enhanced compared to the SM case for light top squarks and large \tilde{A}_t values. Therefore, $\gamma\gamma +$ charged lepton events can be more copious than in the SM, and the contributions of the $pp \rightarrow \tilde{t}\tilde{t}h$ process to these events can render the detection of the h boson much easier than with the process $pp \rightarrow t\bar{t}h$ alone.

4 Conclusions

I discussed the effects of \tilde{t} squarks on the production the lightest neutral SUSY Higgs boson h at the LHC in the context of the minimal supersymmetric extension of the Standard Model.

If the off-diagonal entries in the \tilde{t} mass matrix are large, the eigenstate \tilde{t}_1 can be rather light and at the same time its couplings to the h boson strongly enhanced. The stop loops can then make the cross section times branching ratio $\sigma(gg \rightarrow h) \times \text{BR}(h \rightarrow \gamma\gamma)$, which is the main production and detection mechanism for Higgs bosons at the LHC, much smaller than in the SM, even in the decoupling regime where the h -boson has SM-like couplings to fermions and gauge bosons. [Far from this decoupling limit, the cross section times branching ratio is further reduced in general due to the additional suppression of the htt and hWW couplings.] This will render more delicate the search for the h boson at the LHC with this process.

In this scenario, the process $pp \rightarrow \tilde{t}_1 \tilde{t}_1 h$ can be a copious source of Higgs bosons at the LHC, since the cross section can exceed the one for the SM-like $t\bar{t}h$ production process [for the heavier H and A bosons, the processes are phase space suppressed¹⁵]. This can significantly enhance the potential of the LHC to discover the lightest MSSM Higgs boson in the $l^+\gamma\gamma$ channel. As a bonus, this process would allow to measure the $h\tilde{t}\tilde{t}$ coupling, the potentially largest electroweak coupling in the MSSM, opening thus a window to probe directly the trilinear part of the soft-SUSY breaking scalar potential.

Acknowledgements: I thank the organizing committee, and in particular Joan Solà, for the very nice atmosphere of this fruitful workshop.

References

1. For reviews on the MSSM, see: H.E. Haber and G. Kane, Phys. Rep. 117 (1985) 75; R. Arnowitt and Pran Nath, report CTP-TAMU-52-93; M. Drees and S. Martin, hep-9504324; S. Martin, hep-ph9709356.
2. For a review, see: J.F. Gunion, H.E. Haber, G.L. Kane and S. Dawson, “The Higgs Hunter’s Guide”, Addison-Wesley, Reading 1990.
3. See e.g. H.E. Haber, hep-ph/9505240.
4. PDG, C. Caso et al, Eur. Phys. Jour. C3 (1998) 1.
5. M. Carena, M. Quiros and C.E.M. Wagner, Nucl. Phys. B461 (1996) 407; H. Haber, R. Hempfling and A. Hoang, Z. Phys. C75 (1997) 539; S. Heinemeyer, W. Hollik and G. Weiglein, hep-ph/9803277.
6. ATLAS Collaboration, Technical Proposal, Report CERN-LHCC 94-43; CMS Collaboration, Technical Proposal, Report CERN-LHCC 94-38.
7. For reviews, see e.g.: J.F. Gunion et al., hep-ph/9602238; M. Spira, hep-ph/9705337; Z. Kunszt, S. Moretti and W.J. Stirling, Z. Phys. C74 (1997) 479; A. Djouadi, Int. J. Mod. Phys. A10 (1995) 1.
8. For an update, see: A. Djouadi et al., Eur. Phys. J. C1 (1998) 149.
9. H. Georgi et al., Phys. Rev. Lett. 40 (1978) 692; A. Djouadi, M. Spira and P.M. Zerwas, Phys. Lett. B264 (1991) 440; S. Dawson, Nucl. Phys. B359 (1991) 283; M. Spira et al., Nucl. Phys. B453 (1995) 17; S. Dawson, A. Djouadi and M. Spira, Phys. Rev. Lett. 77 (1996) 16.
10. A. Djouadi, Phys. Lett. B435 (1998) 101.
11. A. Djouadi, J.L. Kneur, G. Moultaka, Phys. Rev. Lett. 80 (1998) 183.
12. A. Djouadi, J. Kalinowski, M. Spira, Comput. Phys. Com. 108 (1998) 56.
13. See for instance, G. Altarelli, hep-ph/9611239.
14. CTEQ Collaboration, Phys. Rev. D51 (1995) 4763.
15. A. Dedes and S. Moretti, hep-ph/9812328; A. Djouadi, J.L. Kneur, G. Moultaka, in preparation.